

# Effect of Rubber Particle Cavitation on the Mechanical Properties and Deformation Behavior of High-Impact Polystyrene

V. Serpooshan, S. Zokaei, R. Bagheri

*Polymeric Materials Research Group, Department of Materials Science and Engineering, Sharif University of Technology, P.O. Box 11365-9466, Tehran, Iran*

Received 9 April 2006; accepted 28 September 2006

DOI 10.1002/app.25633

Published online in Wiley InterScience (www.interscience.wiley.com).

**ABSTRACT:** Rubber particle cavitation has been the focus of many investigations because it dramatically affects the mechanical properties of polymeric blends. In this work, the effect of rubber particle cavitation on the mechanical behavior of high-impact polystyrene was studied. The extent of cavitation in rubber particles was varied via different thermal contraction/expansion cycles in the range of  $-100$  to  $23^{\circ}\text{C}$ . Tensile, creep, and Charpy impact tests were conducted to evaluate the effects of the degree of cavitation on the general mechanical properties. The notch-tip damage

zone and deformation micromechanisms were also investigated by a transmitted optical microscopy technique to reveal the effects of cavitation on toughness. The results of this investigation illustrate a close relationship between the degree of rubber particle cavitation and the mechanical performance of high-impact polystyrene. © 2007 Wiley Periodicals, Inc. *J Appl Polym Sci* 104: 1110–1117, 2007

**Key words:** blends; crazing; damage zone; fracture; mechanical properties; microstructure; polystyrene; toughness

## INTRODUCTION

Although rubber particle cavitation in polymeric blends has been observed for 30 years,<sup>1</sup> the manner in which the phenomenon affects deformation behavior and mechanical properties is still under debate.<sup>2,3</sup> The main obstacles include (1) the limited effectiveness of mechanically induced cavitation methods in studying the effects of cavitation on mechanical properties and (2) the complex salami structure of rubber particles in some polymer blends such as high-impact polystyrene (HIPS). The limited effectiveness of mechanically induced cavitations is due to significant changes in the material properties through the yielding of the matrix, and there are many deficiencies in traditional microscopy techniques for studying mechanically induced cavitation in polymeric specimens because of the disturbing effects of matrix distortion in revealing rubber particles and their substructure.<sup>4</sup> The salami structure in HIPS and the particular manner of cavitation that occurs in such systems (crazelike fibrillation) make the monitoring of the cavitation phenomenon very difficult.<sup>5</sup>

Several studies have been conducted to explore an effective/sensitive method for monitoring rubber particle cavitation in different polymeric blends. In addition to electron microscopy techniques, the limitations

of which have been mentioned previously,<sup>6</sup> some other procedures that have been examined include measuring the intensity of the transmitted light from an incident laser beam (light scattering method),<sup>7</sup> detecting incipient rubber particle cavitation with dynamic mechanical tests,<sup>8</sup> and monitoring dimensional changes through the application of controlled thermal contraction/expansion cycles to specimens to provide a definite degrees of thermally induced cavitation.<sup>4,8</sup> Moreover, some attempts have been made to elucidate the effects of cavitation on the final mechanical properties.<sup>3,7–10</sup> Nevertheless, because of the aforementioned cavitation monitoring restrictions, there is still not a clear understanding of the manner in which cavitation affects mechanical behavior.<sup>2,3</sup>

Among the inducing and monitoring methods of cavitation mentioned previously, the thermal method of inducing cavitation and studying the resulting dimensional changes to monitor cavitation both qualitatively and quantitatively has been more successful, especially in the case of polymeric blends such as acrylonitrile butadiene styrene (ABS) in which large amounts of cavitation occur in the form of single, concentric voids in core-shell particles.<sup>4</sup>

The thermal method for inducing cavitation was developed first by Bucknall and coworkers<sup>4,8</sup> in polymeric blends such as ABS and poly(methyl methacrylate). With this technique, although no deformation occurs in the matrix, rubber particles cavitate in a controlled manner. This cavitation is due to the relatively large thermal stresses that develop between two

Correspondence to: R. Bagheri (rezabagh@sharif.edu).

phases with different coefficients of thermal expansion, generated from contraction/expansion cycles. Different degrees of cavitation can be induced in rubber particles with different cooling temperatures. After a slow return to the ambient temperature, the effects of cavitation on the mechanical properties can be studied in the absence of any disturbing phenomenon.

When a two-phase system composed of a brittle matrix and a rubbery phase undergoes a thermal contraction cycle, above the glass-transition temperature of the rubbery phase, hydrostatic stress ( $\sigma_{hr}$ ) is generated in the system.<sup>4</sup> According to eq. (1), the magnitude of  $\sigma_{hr}$  depends on the difference in the thermal expansion coefficients ( $\beta$ ) of the two phases:

$$\sigma_{hr} = \frac{(\beta_r - \beta_m) \cdot \Delta T}{\frac{1}{K_r} + \frac{4G_m\phi_r + 3K_m}{4G_mK_m(1-\phi_r)}} \quad (1)$$

where  $\Delta T$  is the temperature change applied to the two-phase system,  $G$  and  $K$  stand for shear and bulk moduli, respectively, and  $\phi$  is the volume fraction. Indices  $m$  and  $r$  stand for the matrix and rubber, respectively. In the case of HIPS,  $\beta_m$  is  $1.8 \times 10^{-4} \text{ K}^{-1}$ , and  $\beta_r$  is  $7.6 \times 10^{-4} \text{ K}^{-1}$ .<sup>11</sup> When  $\sigma_{hr}$  reaches the cohesive strength of rubber particles or the adhesive strength at the rubber–matrix interface, then cavitation or debonding will happen, respectively.<sup>12–14</sup> In the case of HIPS, rubber particle cavitation is more likely.<sup>5</sup> This is due to the effective grafting of polystyrene (PS) and polybutadiene chains through a polymerization process that causes higher values of the adhesive strength compared with the cohesive strength of the rubbery phase.<sup>5</sup>

According to eq. (1), while in a thermal contraction/expansion cycle, if a required value of  $\Delta T$  is not maintained, cavitation in the rubbery domains will not happen. On the other hand, if  $\Delta T$  increases so much that the temperature decreases below the glass-transition temperature of the rubbery phase, then both phases will be glassy, and no thermal contraction and expansion will happen to cause further stresses; hence, no cavitation will occur.<sup>14</sup>

To monitor cavitation phenomenon in ABS, Bucknall et al.<sup>4</sup> used a physical procedure by recording the thermal contraction behavior of cooled specimens (normalized specimen length changes,  $\Delta L/L$ ) versus a gradual decrease in the temperature between the ambient temperature and glass-transition temperature of the rubbery phase. When cavitation takes place, an anomalous S-shaped behavior appears in the curve of  $\Delta L/L$  versus the temperature, which implies the occurrence of cavitation (Fig. 1).

Nevertheless, in polymeric systems such as HIPS, with complex salami particles and especially the manner of cavitation mentioned before,<sup>5</sup> merely using the

thermal method of inducing cavitation is not successful. PS membranes with a salami structure inhibit any opening in the system, and so the extent of the cavitation potential in HIPS is generally lower than that of ABS. Therefore, cavitation takes place in such salami systems in the form of numerous, small voids between rubbery fibrils, unlike the large, single cavities in ABS, and this makes the detection and monitoring of cavitation in HIPS a rather difficult job. Therefore, there is a need for an integral method, with a higher degree of sensitivity in comparison with that of the physical procedure used for ABS, to monitor cavitation in HIPS.

In this work, according to the Bucknall procedure, thermal contraction/expansion cycles were incorporated to induce different degrees of cavitation in HIPS specimens. Then, instead of the physical procedure used before for monitoring cavitation, the effects of cavitation on the mechanical properties and plastic deformation behavior were investigated and recorded as an indirect method for monitoring the cavitation phenomenon; hence, the cavitation phenomenon could be monitored more effectively and sensitively, while the effects of such cavitation on the mechanical properties were simultaneously determined.

## EXPERIMENTAL

The materials used in this study were HIPS7240 and HIPS8350, which were manufactured by Tabriz Petrochemical Co. (Tabriz, Iran) and included 8 and 13 vol

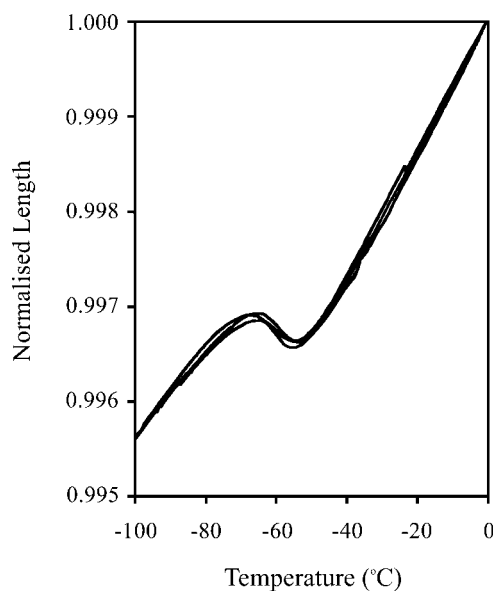


**Figure 1** Thermal contraction behavior of three ABS specimens tested in the  $x$ ,  $y$ , and  $z$  directions.<sup>4</sup> [Reprinted from *Polymer*, Vol. 41, C.B. Bucknall, D.S. Ayre, D.J. Dijkstra, Detection of rubber particle cavitation in toughened plastics using thermal contraction tests, 5937–5947, 2000, with permission from Elsevier.]

TABLE I  
Information About the HIPS Materials

Material	Rubber (vol %)	Yield stress (MPa)	Modulus of elasticity (MPa)	Charpy impact strength (J/cm <sup>2</sup> )
HIPS7240	8	17.0	1872	0.69
HIPS8350	13	15.8	1748	0.81

% rubbery phases with a salami structure (as shown later), respectively. Table I indicates the mechanical properties of the original materials. Thermal contraction/expansion cycles were conducted with a laboratory freezer, which was equipped with liquid nitrogen–alcohol mixtures with different ratios to provide different cooling temperatures. Specimens were cooled to temperatures in the range of  $-100$  to  $23^{\circ}\text{C}$ , held for 1 h, and then returned to the ambient temperature slowly.

All specimens studied in this research were injection-molded at  $250^{\circ}\text{C}$ . Tensile tests were conducted with a Hounsfield H10KS universal frame at a cross-head speed of 5 mm/min. Tensile specimens were prepared according to ASTM D 638. Also, Charpy impact tests were conducted according to ASTM D 256. A Hounsfield H10KS universal frame was also used in creep tests under a constant load of 325 N (on a trial and error basis). Three-point-bending specimens were machined from injected bars measuring  $127 \times 12.8 \times 6.34 \text{ mm}^3$ . A side-edge notch with an angle of  $45^{\circ}$  and a 4-mm depth was machined on each specimen. Three-point-bending tests were carried out until a constant load of 200 N was reached in all specimens (on a trial and error basis). The magnitudes of the deflection of the bent specimens were compared. The notch-tip damage zones of the bent specimens were studied with optical stereomicroscopy, in a transmission mode, to determine the effect of the degree of cavitation on plastic deformation. The optical microscope used in this study was an Olympus BX51. An Olympus SZH10 research stereomicroscope was also used in microscopy studies of the notch-tip damage zones. The specimen thicknesses were polished down to  $75 \mu\text{m}$  before optical microscopy.

To study the real microstructure of the HIPS specimens used in this research and also to verify the cavitation phenomenon that occurred in the cooled HIPS specimens, transmission electron microscopy (TEM) was used. TEM specimens were first trimmed to the size of  $1 \times 1 \times 5 \text{ mm}^3$ . The trimmed blocks were then stained in osmium tetroxide ( $\text{OsO}_4$ ) for about 5 days. The stained blocks were embedded into a low-viscosity epoxy resin before ultrathin (70-nm-thick) slices were cut. Ultramicrotomy was conducted with a Reichert-Jung Ultracut-E equipped with a Diatome  $45^{\circ}$  diamond knife. TEM observations were performed with a Philips CM 200 STEM instrument operated at 200 kV.

## RESULTS AND DISCUSSION

### Mechanical properties

Figure 2 displays the effect of different degrees of cavitation on the yield stress of HIPS7240 and HIPS8350 specimens. The curve of HIPS8350 has been placed below that of HIPS7240. This is due to the higher rubber content in HIPS8350. However, both curves show similar behavior within the thermal range applied. As shown in Figure 2, the yield stress increases gradually with decreasing cooling temperature from the ambient temperature in both materials. In this stage, according to eq. (1), tensile hydrostatic stresses still have not reached the critical cohesive strength of the rubbery phase, and so cavitation still has not taken place. One important factor that has been neglected in previous research in this field is the presence of residual compressive stresses in cooled specimens, in which the hydrostatic stresses [eq. (1)] cannot overcome the cohesive strength of rubber. These stresses put the system in a closing mode and, therefore, postpone crazing in the matrix.

In Figure 2, when the applied value of  $\Delta T$  is not large enough to initiate cavitation [according to eq. (1)], there are only residual compressive stresses built up in the specimens, and those stresses inhibit the formation of crazes in HIPS.<sup>9</sup> Therefore, in this range of temperatures, a lower cooling temperature results in an increasing residual stress level in the system, and so the yield stress increases.

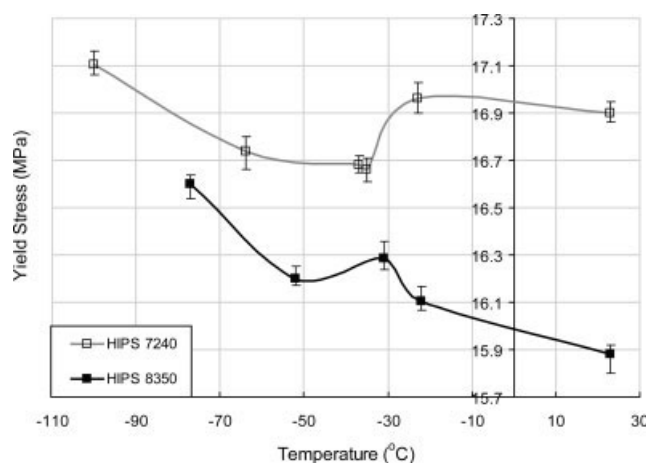
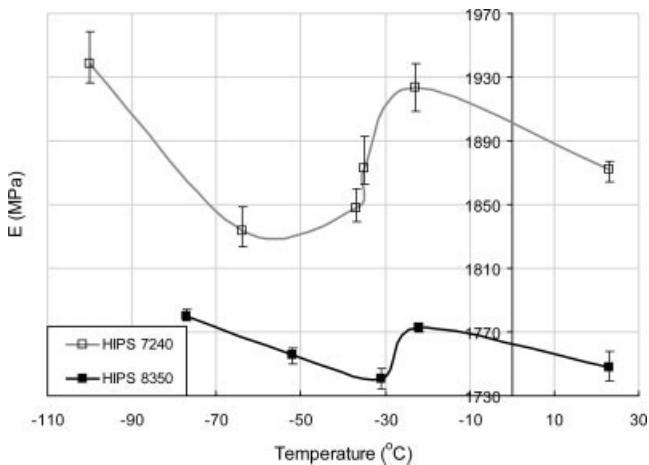


Figure 2 Variation of the yield stress with respect to the cooling temperature for HIPS7240 and HIPS8350.



**Figure 3** Dependence of the elastic modulus ( $E$ ) on the cooling temperature for HIPS7240 and HIPS8350.

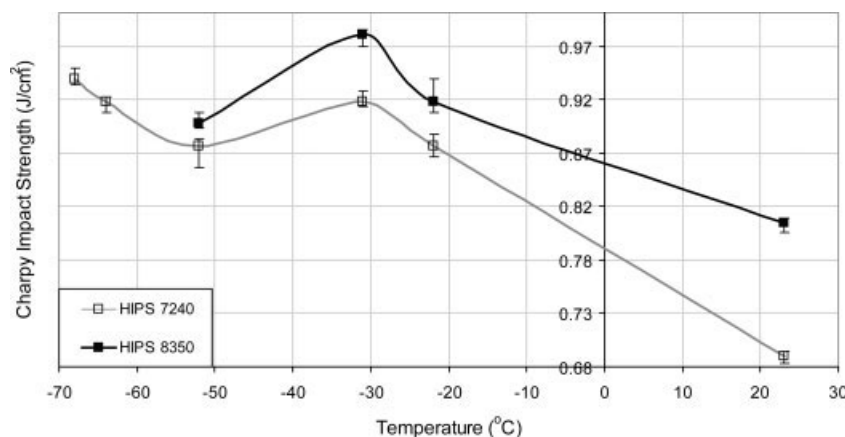
Nevertheless, continuing cooling to about  $-30^{\circ}\text{C}$  results in a sudden drop in the yield stress when the temperature is less than  $-30^{\circ}\text{C}$ . At this point,  $\Delta T$  is large enough that  $\sigma_{hr}$  reaches the cohesive strength of the rubbery phase, and thus cavitation takes place. The presence of preformed cavities in the specimens facilitates yielding of the adjacent matrix in tensile testing because the cavities increase the stress concentration in the adjacent matrix. In fact,  $-30^{\circ}\text{C}$  is a critical/transition point in all cooling cycles; above and below this temperature, different behaviors are observed in the yield stress, modulus, and Charpy impact strength.

An important point to be mentioned here is that at temperatures below  $-30^{\circ}\text{C}$ , it is probable that  $\sigma_{hr}$  in some rubbery domains may not have reached the critical value required to initiate cavitation yet. Therefore, one should consider the effects of cavitation and residual stresses simultaneously and that the compromise between these two factors will determine the final material behavior.

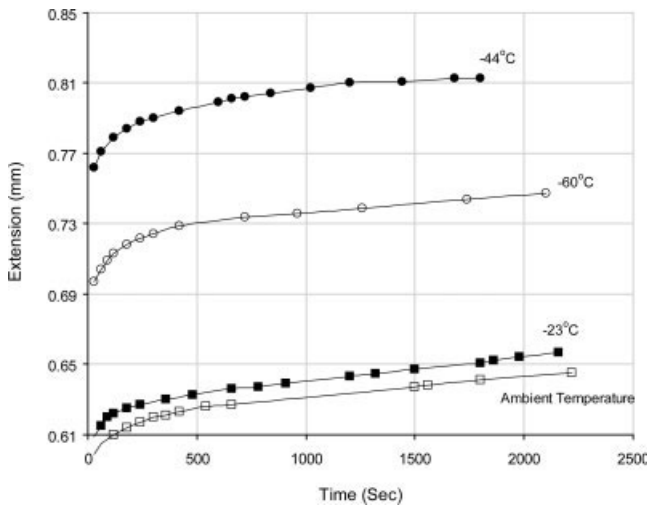
A reduction of the yield stress with cooling continues until  $-55^{\circ}\text{C}$ , at which point the yield stress begins to increase again in both materials. When the cooling temperature comes close to the glass-transition temperature of the rubbery phase, both phases become glassy; therefore,  $\Delta\beta$  in eq. (1) decreases such that  $\sigma_{hr}$ , that is, the driving force for cavitation, is reduced. Therefore, cavitation will gradually diminish in this cooling range, and the effect of the residual stress overcomes the cavitation effect again. This phenomenon is associated with an increase in the yield stress (Fig. 2). In the next subsection, some microscopic evidence is introduced for this proposed hypothesis. TEM micrographs clearly illustrate different cavitation behaviors of HIPS specimens cooled at different temperatures.

Figure 3 shows similar behavior for the elastic moduli of the two materials over the cooling scan. Behavior similar to that observed for the yield stress can be seen for the moduli of elasticity (Figs. 2 and 3). HIPS8350 contains a larger amount of rubber and thus has a lower Young's modulus than HIPS7240. In the first stage, the increase in the elastic modulus as the cooling temperature decreases from the ambient temperature is due to the effect of increasing residual compressive stresses. In the second stage, while cavities form and grow, the modulus begins to decrease. Finally, the gradual termination of cavitation results in increasing modulus when the effect of the compressive stresses prevails again.

In a similar way, the effects of contraction/expansion cycles on the Charpy impact strength of HIPS specimens is displayed in Figure 4. Here, the curve of HIPS8350 is placed above that of HIPS7240 because of improved toughness due to the effects of increased rubber content. Again, at characteristic temperatures (similar to Figs. 1 and 2), the material behavior changes. At first, reducing the cooling temperature from the ambient temperature results in higher levels of compressive stresses and thus higher material resistance against crack propagation and failure. Therefore, the impact strength is increased. Then, as cavitation



**Figure 4** Variation of the Charpy impact strength with respect to the cooling temperature for HIPS7240 and HIPS8350.



**Figure 5** Effect of the thermal cycles on the creep behavior of HIPS7240. All specimens were loaded in tension under a constant load of 325 N.

starts, the impact strength decreases because of the presence of voids in the system, which act as appropriate sites for crack nucleation and growth. At lower cooling temperatures, below  $-55^{\circ}\text{C}$ , the impact strength of HIPS7240 increases again. This is due to the renewed dominance of the compressive residual stresses in the absence of appreciable degrees of cavitation. Similar behavior could be expected for HIPS8350 in this range of temperatures.

Figure 5 presents the effect of thermal cycles on the creep behavior of HIPS7240. The creep curve of the specimen cooled at  $-23^{\circ}\text{C}$  is placed so close to that of the ambient temperature that it implies that there is no effect of residual stresses on this cooled specimen. Nevertheless, lowering the cooling temperature from the ambient temperature to  $-44^{\circ}\text{C}$  results in increasing creep deformation. A further reduction in cooling temperature from  $-44$  to  $-60^{\circ}\text{C}$ , however, reduces the magnitude of the creep deformation because of the gradual termination of cavitation. These two curves imply the effect of cavitated particles in facilitating plastic deformation (crazing) in the matrix. An important observation here is the absence of an effect of the residual compressive stresses on the plastic deformation of all cooled specimens; this is especially obvious in the case of the specimen cooled at  $-23^{\circ}\text{C}$ , when there should be only the effect of these compressive stresses. Because creep tests in this research were conducted under a constant load of 325 N, all residual stresses were omitted during the application of this constant load; hence, there is no effect of residual stresses here.

Another experiment carried out in this research was a three-point-bending test of notched bars up to a constant load of 200 N. Figure 6 shows the results of this experiment for cooled HIPS7240 specimens. With cooling from the ambient temperature to  $-20^{\circ}\text{C}$ , the load–displacement curve shifts to the left. Although the shift is not

very significant, it still shows that the cooled material is stiffer than the control specimen. This observation might be attributed to the effect of compressive stresses built up within this temperature range that inhibit deformation at the notch tip of the bending specimen. Further cooling specimens to  $-34^{\circ}\text{C}$ , as shown in Figure 6, makes the material more compliant. This observation implies that cavities formed at  $-34^{\circ}\text{C}$  reduce the stiffness of the material and ease deformation at the notch tip of the bending specimen. This effect is more pronounced in the specimen cooled at  $-57^{\circ}\text{C}$ , at which the material yields below a 170 N load because of a higher degree of cavitation (Fig. 6).

### Microscopy evaluation

Figure 7(a,b) shows TEM micrographs of HIPS7240 and HIPS8350 microstructures, respectively. The salami substructure in both HIPS materials can be seen clearly. Figure 8(a–c) shows TEM micrographs of HIPS7240 specimens undergoing cooling cycles at  $-20$ ,  $-40$ , and  $-70^{\circ}\text{C}$ , respectively. In Figure 8(a,c), no evidence of cavitation can be seen, and the rubbery domains between the PS subinclusions are intact and solid, whereas in Figure 8(b), cavitated particles are clearly visible in the form of fibrillated, rubbery domains surrounded by solid PS subinclusions. This is microscopic proof of the hypothesis explained previously for the influence of the cooling temperature on the mechanical behavior of HIPS. Between two characteristic transition temperatures for HIPS materials in this study (ca.  $-30$  and  $-55^{\circ}\text{C}$ ), cavitation takes place to a significant degree [Fig. 8(b)], whereas above and below this temperature range, residual compressive stresses due to cooling cycles have relative dominance

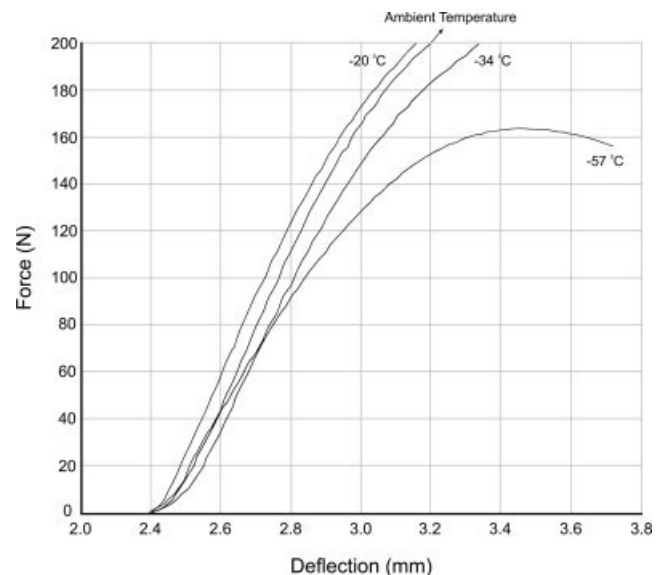


**Figure 6** Load–displacement curves for HIPS7240 specimens obtained in three-point-bending experiments.

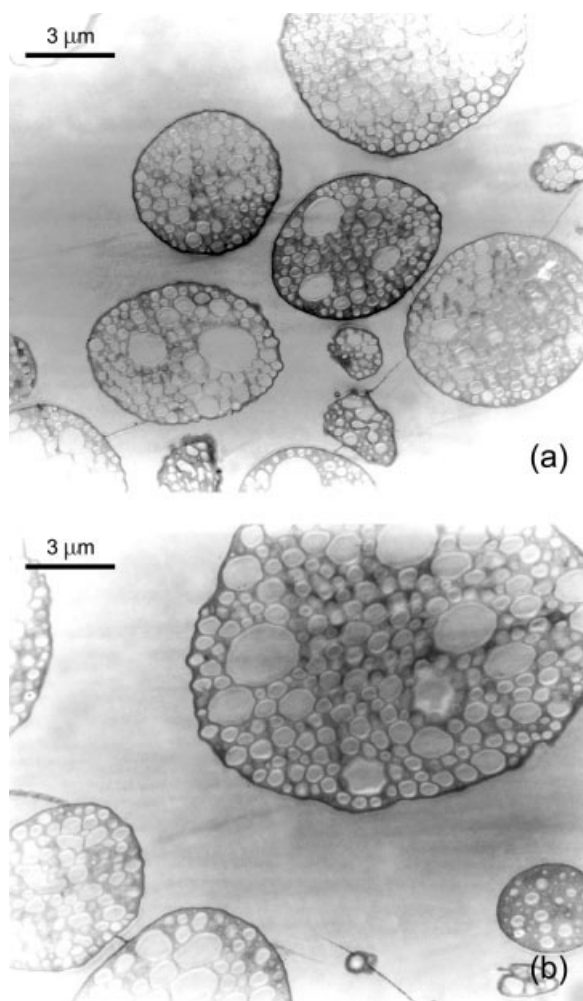
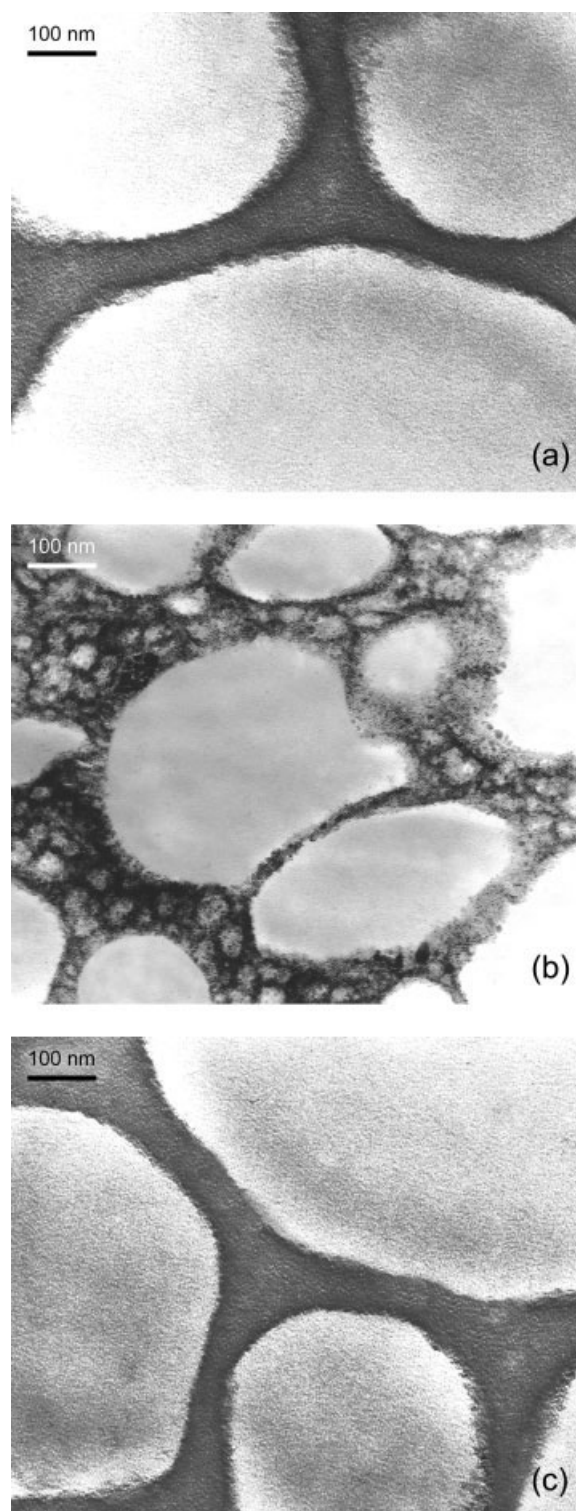


**Figure 7** TEM micrographs of (a) HIPS7240 and (b) HIPS8350 specimens. The salami substructure of the second phase can be clearly seen in both materials.

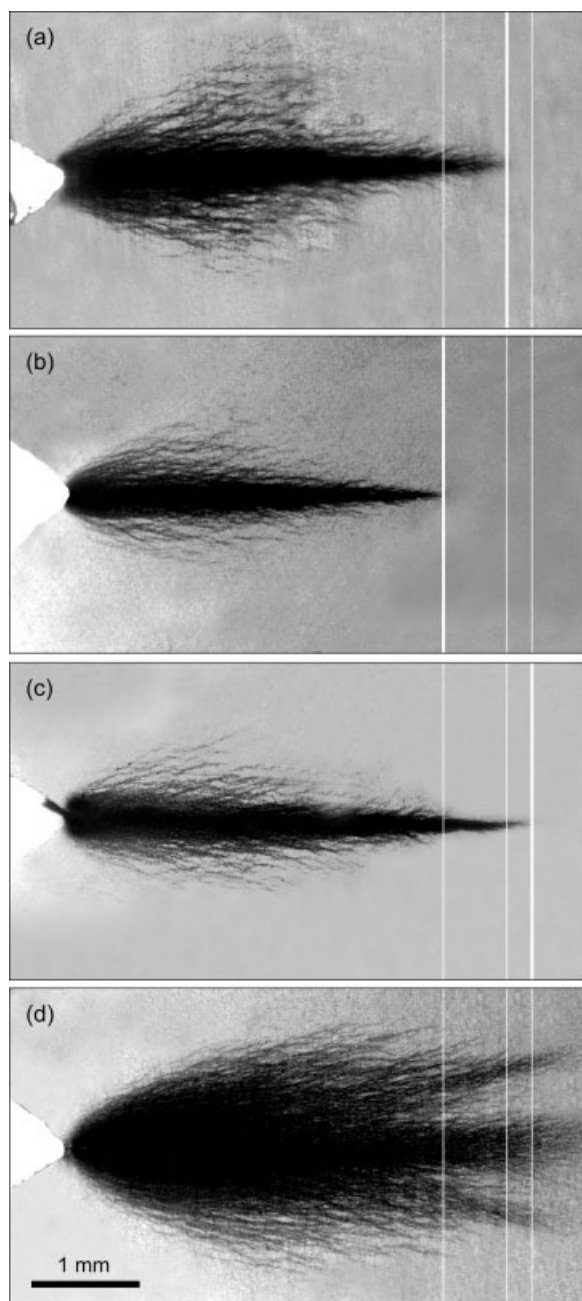
against cavitation; hence, there is no effective cavitation taking place in the system [Fig. 8(a,c)].

Figure 9 shows notch-tip damage zones of the same bent specimens obtained via optical stereomicroscopy in a transmission mode. The white lines indicate the damage-zone front tips to enable the reader to compare the sizes of the plastic deformation zones at different temperatures. Comparing Figure 9(a,d), we can conclude that as the specimens are cooled from the ambient temperature, the damage-zone size initially decreases because of the compressive stresses that suppress cavitation. Then, with a further decrease in the cooling temperature below  $-57^{\circ}\text{C}$ , the extent of cavitation increases, and the damage zones become extended. With an increasing degree of cavitation, the size of the damage zone and its branches increase considerably. Figure 10 explains this phenomenon in more detail. Figure 10(b) shows a specimen cooled at  $-20^{\circ}\text{C}$ , in which crazes are less dense with respect to the ambient temperature [Fig. 10(a)], whereas in Figure 10(c), for the specimen cooled at  $-57^{\circ}\text{C}$ , the density of crazing has been increased dramatically. Also,

in Figure 10(c), crazes appear clearly finer with respect to Figure 10(a,b). This implies the facilitating effect of cavitation in the yielding micromechanism of HIPS.



**Figure 8** TEM micrographs of HIPS7240 specimens cooled at (a)  $-20^{\circ}\text{C}$ , (b)  $-40^{\circ}\text{C}$ , and (c)  $-70^{\circ}\text{C}$ . Although no evidence of cavitation can be seen in parts a and c, cavitation in the form of a crazelike, fibrillated, rubbery domain between PS subinclusions can be seen in part b.



**Figure 9** Optical micrographs of notch-tip damage zones in HIPS7240 specimens at different temperatures: (a) 23, (b)  $-20$ , (c)  $-34$ , and (d)  $-57^{\circ}\text{C}$ .

Regarding Figures 9(b) and 10(b), in comparison with Figures 9(a) and 10(a), can provide proof for the presence of compressive residual stresses in  $-20^{\circ}\text{C}$  cooled specimens and their effect on postponing cavitation and successive crazing in the HIPS specimens.

#### Effect of cavitation on the fracture toughness

With an increasing cavitation degree in cooled HIPS specimens, the Charpy impact strength decreases, but the notch-tip damage zones in three-point-bending

specimens become more extended (Figs. 9 and 10). A comparison of induced damage zones at the notch tip before the fracture of HIPS7240 specimens tested under an impact loading rate (in a Charpy test) and a quasi-static loading rate (in a three-point-bending test) is shown in Figure 11. With high loading rates, such as the loading rate in impact tests, HIPS materials behave in a brittle manner, and a very narrow damage zone forms around the fracture surfaces [Fig. 11(a)]. In this case, not only is the effect of preformed cavities in facilitating deformation not effective enough in energy absorption, but these cavities also act as suitable nucleation sites for crack initiation; hence, increasing the cavitation degree

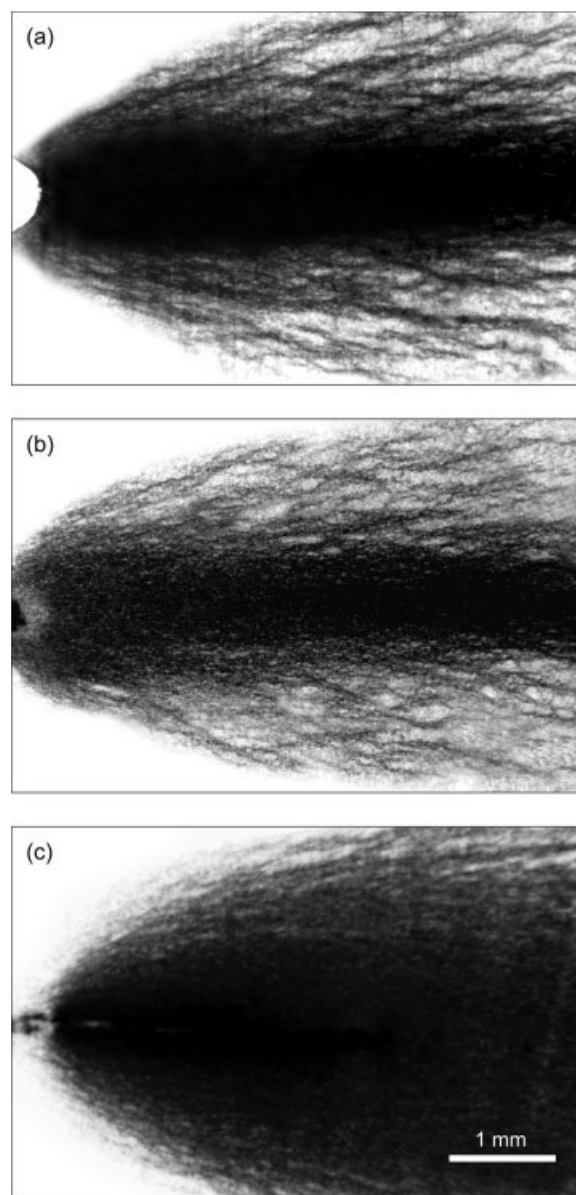


**Figure 10** Optical micrographs of notch-tip damage zones (a higher magnification of Fig. 7) in HIPS7240 specimens cooled at different temperatures: (a) 23, (b)  $-20$ , and (c)  $-57^{\circ}\text{C}$ .

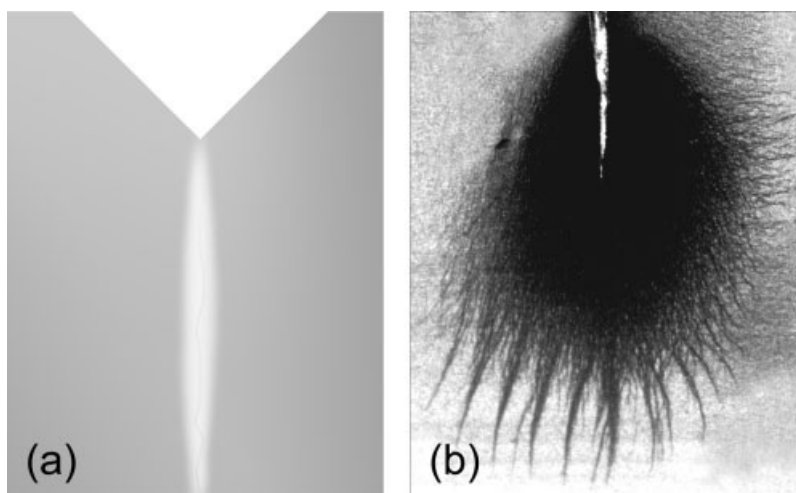


**Figure 11** Comparison of the damage zones at the notch tip before fracture in HIPS7240 specimens undergoing (a) Charpy impact testing and (b) three-point-bending testing obtained via optical microscopy.

reduces the impact strength. However, with lower loading rates, such as the loading rate applied in three-point-bending tests, HIPS is more ductile, and large notch-tip damage zones form [Figs. 9, 10, and 11(b)]. These observations imply that cavitation here is an effective energy absorption mechanism, and so increasing the cavitation degree will result in increasing fracture toughness with quasistatic loading rates.

### CONCLUSIONS

It is concluded that thermally induced cavitation is a suitable method for monitoring the influence of rubber particle cavitation on mechanical properties in polymer blends such as HIPS. In general, the results of this investigation can be summarized as follows:

- There are two important factors affecting the mechanical properties of polymer blends in thermal contraction/expansion testing: rubber particle cavitation and residual compressive stresses, which act as inverses of each other.
- A compromise between the cavitation degree and residual stresses will dominate the final behavior of the material in all mechanical and microscopic aspects.
- The evaluation of the mechanical properties of the treated specimens reveals that in all cases, a uniform behavior was obeyed, and this was the result of a balance between the two engaged factors mentioned previously.
- A microscopic evaluation of the plastic deformation behavior of HIPS specimens reveals that applying thermal contraction/expansion cycles dramatically influences the extent of crazing, the shape of the damage zone, and the size of individual crazes.
- An exact relationship between the microscopic observations and the changes in the mechanical

properties through different thermal contract/expansion cycles has been established.

- Although increasing the cavitation degree results in a fracture toughness increase, it also results in an impact strength decrease. Therefore, an optimum degree of the cavitation potential can be determined for HIPS parts, depending on the different service conditions for each one.

Studying the effect of rubber particle cavitation in other polymer blends to identify similar evidence could be the subject of future studies. Also, at this time, the incorporation of the essential work of the fracture method, to evaluate the changes in the fracture toughness of HIPS specimens cooled at different temperatures, is the subject of our current study.

### References

1. Bascom, W. D.; Cottingham, R. L.; Jones, R. L.; Peyser, P. J. *J Appl Polym Sci* 1975, 19, 2545.
2. Katime, I.; Quintana, J. R.; Price, C. *Mater Lett* 1995, 22, 297.
3. Ramsteiner, F.; Heckmann, W.; McKee, G. E.; Breulmann, M. *Polymer* 2002, 43, 5995.
4. Bucknall, C. B.; Ayre, D. S.; Dijkstra, D. J. *Polymer* 2000, 41, 5937.
5. Bucknall, C. B. In *Polymer Blends*; Paul, D. R.; Bucknall, C. B., Eds.; Wiley: New York, 2000; Vol. 2, Chapter 22, p 101.
6. Rios-Guerrero, L.; Keskkula, H.; Paul, D. R. *Polymer* 2000, 41, 5415.
7. Dijkstra, K.; Van Der Wal, A.; Gaymans, R. J. *J Mater Sci* 1994, 29, 3489.
8. Bucknall, C. B.; Rizzieri, R.; Moore, D. R. *Polymer* 2000, 41, 4149.
9. Bucknall, C. B.; Soares, V. L. P. *J Polym Sci* 2004, 42, 2168.
10. Correa, C. A.; de Sousa, J. A. *J Mater Sci* 1997, 32, 6539.
11. Brandrup, J.; Immergut, E. H. *Polymer Handbook*, 4th ed.; Wiley: New York, 1999; pp v/2, v/91.
12. Ayre, D. S.; Bucknall, C. B. *Polymer* 1998, 39, 4785.
13. Lazzeri, A.; Bucknall, C. B. *J Mater Sci* 1993, 28, 6799.
14. Bucknall, C. B.; Karpodinis, A. M.; Zhang, X. C. *J Mater Sci* 1994, 29, 3377.